THE JOURNAL OF PHYSICAL CHEMISTRY B

ARTICLE

pubs.acs.org/JPCB

Size and Charge Modulation of Surfactant-Based Vesicles

Aurelio Barbetta,[†] Carlotta Pucci,[†] Franco Tardani,[†] Patrizia Andreozzi,[‡,||] and Camillo La Mesa[*,†,§]

[†]Department of Chemistry, La Sapienza University, Rome, Italy

[‡]Italian Institute of Technology, Lecce, and [§]Soft-INFM, La Sapienza University, Rome, Italy

ABSTRACT: Nonstoichimetric mixtures of two oppositely charged surfactants, such as sodium dodecylsulfate and hexadecyltrimethylammonium bromide or tetradecyltrimethylammonium bromide and tetraethylammonium perfluorooctanesulfonate, a fluorinated species, form vesicles in dilute concentration regimes of the corresponding phase diagrams. Vesicles size and charge density are tuned by changing the mole ratio between oppositely charged species, at fixed overall surfactant content. They are also modulated by adding neutral electrolytes, or raising *T*. In the investigated regions, mixtures made of sodium dodecylsulfate/hexadecyltrimethylammonium bromide show ideality of mixing, the other non ideality and phase separation. The formation of unilamellar vesicles occurs in the sodium dodecylsulfate/hexadecyltrimethylammonium bromide mixture, but not in the other. DLS, viscosity, and electrophoretic mobility quantified the above effects. Surface charge density, surface tension, elasticity, and osmotic pressure concur to the stability of unilamellar vesicles and a balance between the above contributions is demonstrated. The results are relevant for practical applications of vesicles as carriers in biomedicine.

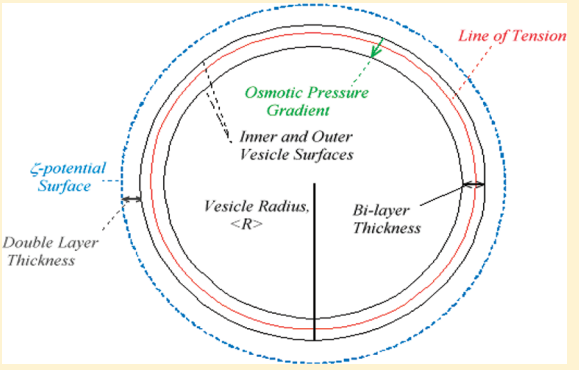

1. INTRODUCTION

Much interest is currently devoted to the physical chemistry of surfactant mixtures.[1−5] The reasons why the scientific community pays attention on these mixtures find justification in formulation-devoted applications.[6−9] In water-based media, the rational use of surfactant mixtures offers the opportunity to modulate the molecular packing constraint of each surface active species,[10] and to prepare supra-molecular aggregates with "ad hoc" size, shape and charge density.[11] The tailored properties of the mixed aggregates have consequences on technological performances in many practical applications, including biologically oriented ones.

Focus is on systems obtained by mixing oppositely charged surfactants. Because of the substances from which are made of, the systems are termed cat/anionic.[12,13] Changes in the aggregate size and charge densities are observed upon mixing, and surfactant-based vesicles do form in the corresponding phase diagrams.[14,15] The properties of such aggregates are the result of chain mixing, packing into entities with peculiar physical state compared to the single components, and polar head/counterion or ion/ion interactions at their surfaces. It is easy to find stable, or charge-stabilized, cat/anionic vesicles in part of the phase diagrams.[16,17]

At present, it is not known whether the stability of cat/anionic vesicles is of thermodynamic or kinetic nature. When some unilamellar vesicles are equilibrium structures,[18−20] the case of multilamellar ones, which exist in far from equilibrium conditions and phase separate with aging, is controversial. The former vesicles are easy to handle in thermodynamic modeling, and the approach we report here applies to such cases.

Experiments focus on the size and surface charge density of cat/anionic vesicles and deal with the forces controlling the stability of such dispersions. Mixtures are made by mixing sodium dodecylsulfate and hexadecyltrimethylammonium bromide,[21] or tetradecyltrimethylammonium bromide, and tetraethylammonium perfluorooctanesulfonate.[22] The former system is termed SDS/CTAB, the latter TTAB/TEAPFOS. Both form vesicles in part of the corresponding phase diagrams, in dilute concentration regimes.

In this contribution the effects that mixture composition, temperature and ionic strength play in vesicle formation are dealt with. Experiments focus on the size and surface charge density of cat/anionic vesicles and deal with the forces controlling the kinetic, or thermodynamic, stability of such dispersions. We discuss the effect that added salt and temperature, or combinations thereof, have on the association features of these vesicular systems and report on the formation of unilamellar entities. Multilamellar vesicles are metastable, but may form stable bilayers by raising the temperature. Very presumably, the effect is governed by matter exchange between concentric bilayers and by the subsequent change in size up to reach a "quasi critical" point.[23] Thereafter, vesicles get such state and retain an equilibrium size, even after a prolonged stay at room temperature.

The manuscript describes some phenomena observed in mixtures with "ideal" mixing between alkyl chains, as the SDS/CTAB one, and the "non ideal" TTAB/TEAPFOS system, respectively. Efforts were made to find rational explanations to the stability of unilamellar vesicles, obtained upon heating the dispersions.

Received: March 4, 2011
Revised: September 15, 2011
Published: September 15, 2011

The stability of unilamellar vesicles is ascribed to the balance of different forces, jointly concurring to the system stability. Experimental evidence comes from DLS, surface tension, viscosity and electrophoretic mobility. The consequences associated to the observed effects are outlined and rationalized. Applications of the model are possible in biologically oriented areas, since unilamellar vesicles interact with oppositely charged biomacromolecules and act as carriers in drug delivery technologies.[24−26]

2. EXPERIMENTAL SECTION

2.1. Materials. Sodium dodecylsulfate, SDS, tetraethylammonium perfluorooctanesulfonate, TEAPFOS, tetradecyltrimethylammonium bromide and hexadecyltrimethylammonium bromide, TTAB and CTAB, were from Sigma. Purification was made by dissolution in hot ethanol, filtration and precipitation by cold acetone. The procedure was repeated twice and the final powders were vacuum-dried at 70 °C. Determination of the CMC and Krafft temperature, T_K, for each surfactant were used as a purity criterion.[27,28] Conductivity water ($\chi < 10^{-7}$ Ω^{-1} cm^{-1} at 25.00 °C) was prepared by distillation in alkaline $KMnO_4$. Ethanol and acetone (Sigma) were of synthetic grade. Salts used to modulate the effect of ionic strength are NaBr in the SDS/CTAB system and TEABr, tetraethylammonium bromide, in the TTAB/TEAPFOS one, respectively. The salts, from Sigma, were vacuum-dried at 70 °C before use.

2.2. Material Preparation. The dispersions were prepared by mixing aqueous SDS and CTAB, or TTAB and TEAPFOS, solutions at T values higher than the T_K of the less soluble species in each mixture (N.B. 1.0−1.0 cat/anionic salt-free mixtures, not dealt in this context, have high Krafft point[29]). Nonstoichiometric vesicles are steadily formed, as inferred by a fast increase in the dispersions turbidity. For properly tuned mole ratios no sedimentation, phase separation, or birefringence could be observed, even after long-term equilibration times. A tendency to phase separate was met at temperatures lower than 20 °C, with precipitation of the components.

The concentrations are located in a range where vesicle stability is effective. The overall surfactant content of SDS/CTAB mixtures is 6.0 mmol kg^{-1}. In the SDS-rich side of the phase diagram, charge-density modulation is obtained by changing the mole ratio SDS/CTAB from 1.1/1.0 to 3.4/1.0. Mixtures are allowed to stay at room temperature for weeks; no sonication is needed. Heating−cooling cycles ensure the formation of stable unilamellar vesicles. TTAB/TEAPFOS mixtures contain an overall surfactant content of 10.0 mmol kg^{-1}; the optimal mole ratio is in the range 4.0/1.0−1.5/1.0. Stirring or sonication were not used. Heating has a moderate effect on vesicle size and is immaterial in the formation of unilamellar entities. Vesicles occur only for certain proportions between the components.

The vesicular dispersions were prepared in water and NaBr for the SDS/CTAB system, in water and TEABr for the other, respectively. Salts were added in solid form, soon after mixing the surfactant solutions. The above procedure improves the stability of the dispersions and ensures a tailored osmotic control to vesicle size.

2.3. Methods. *2.3.1. Dynamic Light Scattering.* A Zeta Nanosizer unit, Malvern, performed DLS measurements at 632.8 nm, in back scattering mode (BSM), at 173°. The BSM configuration minimizes multiple scattering effects and allows measuring polydisperse systems. The apparatus performances were checked by standard procedures.[30] Thermal equilibrium was controlled by a Peltier facility, operating in the range 25.0−65.0 °C. Cells were cleaned and washed with bidistilled water. The solutions were passed through 0.80 μm Millipore filters and equilibrated at 25.0 °C.

Correlation fits of the scattering intensity, $I(t)$ versus log t, (where t is in μs) were elaborated by CONTIN algorithms.[31,32] The autocorrelation function, $g1(\tau)$, determined the apparent self-diffusion coefficient, D_{app} The hydrodynamic radii were evaluated by the Stokes−Einstein equation. The uncertainty on particle sizes ranged around 0.2−0.3 nm for micelles and 10−20 nm for vesicles.

Additional experiments were run as a function of scattering angle. The vertically polarized laser light passes through a pinhole, is focalized in the cell (at 25.0 ± 0.05 °C), passes through the sample, and reaches a 2030 AT photomultiplier (Brookhaven Instruments, Redditch, Worchestershire, U.K.), located on a rotating arm. The position of the diffusion angle is selected by a 200 MS goniometer (Brookhaven Instruments, Redditch, Worchestershire, U.K.). Measurements were run at 45, 90, 120, 135, and 150°.

2.3.2. Electrophoretic Mobility. A laser-Doppler unit determined the surface charge density, σ, of vesicles moving under an applied electric field, $\overline{E}$.[33] Measurements were run at the required temperature in cells equipped with gold electrodes located at 3.0 mm aloof. The scattered light passing in the medium, subjected to the action of $\overline{E}$, undergoes a frequency shift compared to unperturbed conditions. The shift is elaborated, to give the electrophoretic mobility, μ, and the ζ-potential. The latter can related to an electric moment per unit area.[34] The uncertainty on ζ-potentials is in the range 0.5−1.0 mV.

2.3.3. Viscosity. Measurements were run by Ubbelohde viscometers having flow times for the solvent, $t°$, close to 250 s. They were located in a water bath at 25.00 ± 0.02 °C, or at different temperatures, if required. Five individual measurements were run for each point, and the uncertainty on flow times is <0.5 s. In the two-phase area of TTAB-TEAPFOS mixtures the uncertainty on flow times is much higher. The viscosity of the dispersions was taken relative to the solvent (water or brine), according to $\eta_{rel} = (t\rho/t°\rho°)$, where ρ and $\rho°$ are the solution and solvent densities, respectively.

2.3.4. Density. Density, ρ, of the solutions and dispersions was measured by an Anton Paar DMA 60 unit, at the same temperatures as in viscosity experiments. The nominal accuracy on density values is to $\pm 5 \times 10^{-6}$ g cm^{-3}.

2.3.5. Surface Tension. It was measured by a Kruss K10T unit, equipped with a Du Nouy platinum ring, previously flamed, cleaned with 1.0 m HCl, and washed with bidistilled water. Unless otherwise stated, the measuring temperature is 25.00 ± 0.02 °C. Doubly distilled water, γ = 72.0 dyn cm^{-1}, and absolute ethanol, γ = 21.8 dyn cm^{-1}, at 25.0 °C,[35] were used to calibrate the measuring unit.

In the preparation of dispersions, micellar solutions of one component were added with due amounts of the other. To minimize drifts in adsorption kinetics, measurements were run 10 min after addition of each aliquot. The reported γ values are the average of five runs and the related accuracy is to ±0.1 dyn cm^{-1}. Measurements as a function of temperature were performed from 25.0° to 60.0 °C in 5.0 °C steps. Data in Figure 1 indicate that vesicular dispersions are more surface active compared to the mixtures from which are made of, and that their thermal drift ($\partial\gamma/\partial T$), is moderate.

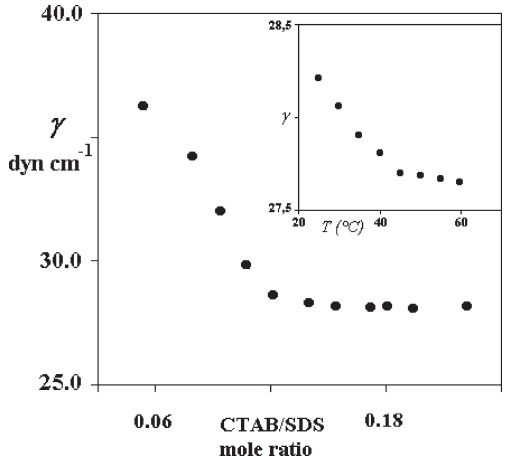

Figure 1. Surface tension, γ (dyn cm^{-1}) of 6.0 mmol surfactant mixtures vs the *CTAB/SDS* mole ratio. Vesicles occur above the change in slope. The inset refers to the temperature dependence of γ values in a mixture made of 3.6 mmol SDS and 2.4 mmol CTAB.

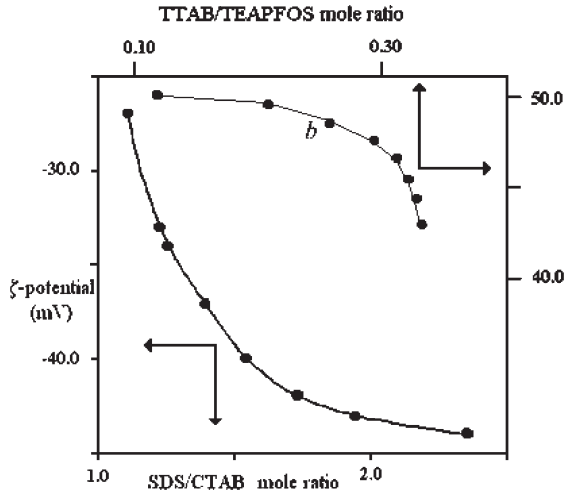

Figure 2. Dependence of ζ-potential values (in mV) versus mole ratio for the SDS/CTAB system, curve a, and the TEAPFOS/TTAB one, curve b, at 25.0 °C.

3. RESULTS

The macroscopic properties of the systems considered here share some points in common and significant differences. They cannot be evaluated on the same grounds. In fact, hydrocarbon-based amphiphilic mixtures have different properties compared to hydrocarbon-fluorocarbon ones,[36,37] and nonideality of mixing is a rather common feature.[38−40] This is why the two systems are discussed separately.

3.1. SDS/CTAB System. The cationic rich side and the region close to the 1.0/1.0 mol ratio were not investigated in detail, since two-phase areas and precipitates were met. At 25.0 °C and in the SDS-rich area, vesicles diameters, $2R_H$, scale with the mole ratio between the components. They increase from 300 to about 700 nm on approaching the 1.0/1.0 ratio.[26,34] In Figure 2 is reported the dependence of ζ-potential on the mole ratio. ζ-potentials tend to zero on approaching the above ratio (which is also a charge neutralization threshold).[26,34]

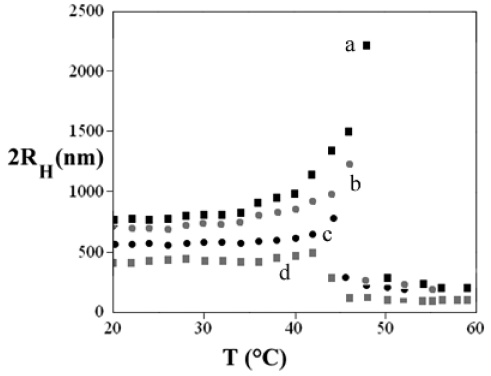

Figure 3. Dependence of average vesicle diameter, $2R_H$, (nm), on T, in °C, for 1.7/1.0 (a), 2.4/1.0 (b), 2.6/1.0 (c), and 2.8/1.0 (d), SDS/CTAB mole ratios, respectively.

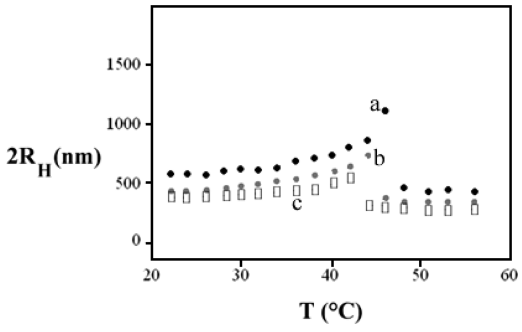

Figure 4. Dependence of the average vesicle diameter, $2R_H$, in nm, on T, in °C, for a 6.0 mmol SDS/CTAB mixture of mole ratio 2.4/1.0 (a). In the plot are also reported data for the same system in presence of 10.0, (b), and 25.0 mmol NaBr, indicated as (c).

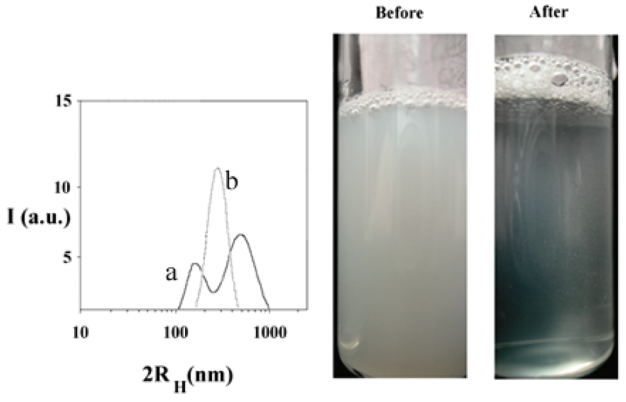

Figure 5. Macroscopic appearance of a 6.0 mmol SDS/CTAB mixture (of mole ratio 2.5/1.0), before and after thermal cycling. The mixture was heated to 50.0 °C and then equilibrated at room temperature. The slightly opalescent character is retained for long times. In the left-hand side is reported the distribution of diameters, I (nm), vs $2R_H$ before (a) and after thermal cycling (b).

Increasing T has a large effect on vesicle sizes, which drastically increase up to a critical and concentration dependent transition temperature, Figure 3. Above that point, indicated as T^*, vesicle size diverges, levels off and does not change. As indicated in Figure 3, T^* scales with the SDS/CTAB mole ratio and decreases

with the relative amount of SDS. The same holds for vesicle sizes at T^*. Added electrolyte modifies the observed trends and shifts T^* to lower values, Figure 4.

Thermal transitions are macroscopic in character and can be determined by the naked eye. Above T^*, the turbidity is much lower than below, Figure 5. The narrow size distribution of unilamellar entities obtained by thermal cycling is centered around 200−300 nm (inset in Figure 5). When they are kept at room temperature, the opalescent character of thermally conditioned dispersions is retained for long times; the same holds for their size. In such conditions vesicles are in unilamellar state.[23] Once such state is reached, the resulting dispersions remain stable. Thermally conditioned vesicles retain the unilamellar state, provided the working temperature is close to 20−22 °C; below that limit, phase separation occurs.

Vesicle growth is presumably related to the differential entropy of transfer of the components between vesicles and the bulk. The process ends when the partition is completed. The effect is particularly relevant for SDS, which is more easily partitioned toward the bulk compared to CTAB. The above statements finds support from experiments. In fact, ζ-potential data significantly decrease (in modulus) by raising T. Changes in ζ-potential by raising T imply possible changes in vesicle composition, curvature and surface tension.

Surface work is due by the chemical potentials of the species, according to

$$d\gamma = -\sum i\Gamma_i \, d\mu_i \qquad (1)$$

where μ_i is the chemical potential of the ith species and Γ_i is inversely proportional to the area per molecule. In the region of existence of vesicles, the surface tension is significantly lower than the one of the surfactants from which they are made. Despite the significant changes observed in vesicle size, $(\partial\gamma/\partial T)$ values are low, in line with previous studies on surfactant mixtures.[41] The reason for that can be ascribed to the concomitant decrease in the observed surface charge density.

Differentiation of eq 1 with respect to T gives

$$\left(\frac{\partial\gamma}{\partial T}\right) = -\left[\sum_i \Gamma_i\left(\frac{\partial\mu_i}{\partial T}\right) + \sum_i \partial\mu_i\left(\frac{\partial\Gamma_i}{\partial T}\right)\right] \qquad (2)$$

and indicates modifications in both surface area, $(\partial\Gamma_i/\partial T)$, and in the partial molal entropy of each component, $(\partial\mu_i/\partial T)$. If a relation between surface tension and charge density holds, that is, $d\gamma = -\sigma \, d\Psi$ (where Ψ is the potential due to all ionic species around a charged vesicle), eq 2 indicates that thermally induced changes in surface tension imply variations in charge density. Thus, ion adsorption onto vesicles and surface charge density are entropy-controlled.

It is not straightforward to define the concentration of each species in the inner and outer vesicle layers, but tentative hypotheses can be done. In case of 1/1 stoichiometry, the surfactants pack into lamellar entities, with zero net charge, and the corresponding mixtures precipitate out. In that case the composition in the two layers is nearly the same. When the SDS/CTAB mole ratio is >1, as in the present system, negatively charged vesicles occur. The distribution of the two species in the inner and outer bilayers can be rationalized in terms of curvature-dependent effects. For such mole ratios the inner layer contains, in proportion, more CTAB than the outer, because of the aggregate curvature and of the spontaneous packing constraint of the components into vesicles. We assumed that the component with higher packing parameter, CTAB, is preferentially located in the inner vesicle layer, in proportion to its spontaneous packing parameter, V/Al.[10] There, V is the alkyl chains volume, A the molecular area at the interface and l the alkyl chain length in fully extended conformation.

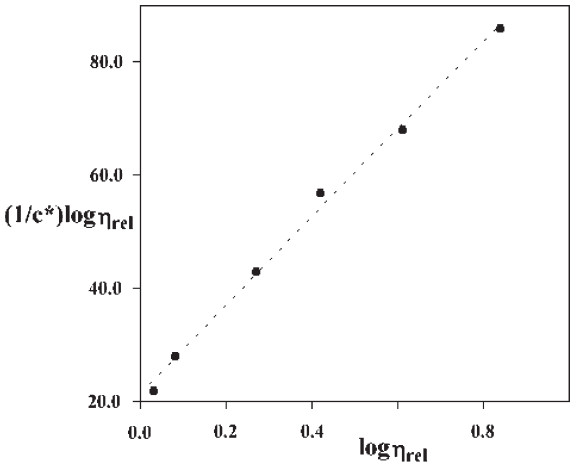

Figure 6. Vand's plot of the function $[1/c^*]\log \eta_{rel}$ (mol kg^{-1}) versus $\log \eta_{rel}$, calculated by eq 3, for pure TEAPFOS micelles, at 25.0 °C.

3.2. TTAB/TEAPFOS System. DLS and viscosity determined the behavior in TEAPFOS/TTAB mixtures, in water or with added TEABr. In this system micelles or vesicles occur, depending on the mole ratio between the components. Sizes of vesicles or micelles in that system do not scale with composition. For TEAPFOS/TTAB mole ratios between 0.40 and 0.60, significant turbidity and formation of precipitates is observed. Very presumably, the significant difference in alkyl chain length of the two species do not allow an optimal packing efficiency, which depends on the length ratio between hydrocarbon and fluorocarbon alkyl chains. The poor chemical affinity between the two components plays a pivotal role in phase separation.[42] Fluororocarbon−hydrocarbon surfactant mixtures show large departures from the ideality of mixing, with phase separation and demixing.[43] Another reasons for the observed behavior is due to the bulkiness and rigidity of fluorinated chains compared to hydrocarbon-based ones. This effect modifies the bilayer elasticity.

Perfluorinated surfactants in solution may form non spherical micelles.[44] To account for that behavior, DLS investigation on micellar TEAPFOS was complemented by viscosity data. The latter were expressed in terms of Vand's equation,[45,46] according to

$$\left(\frac{1}{c^*}\right)\log \eta_{rel} = A_\eta + B_\eta \log \eta_{rel} \qquad (3)$$

where c^* is the concentration of surfactant in micellar form ($c^* = C_{tot}$ − CMC; the CMC of that species is 1.13 mmol kg^{-1}, at 25.0 °C), and A_η the related hydrodynamic volume. B_η accounts for interactions between micelles and is controlled by the Brownian motion. Changes in slope of the function in eq 3 are concomitant to size and shape transitions. No such behavior was observed, Figure 6. That is, TEAPFOS aggregates do not change in shape. A similar behavior was also met in DLS experiments.

In the TEAPFOS/TTAB mixed micellar system, anisometric aggregates may occur. We tried to determine if the above hypothesis holds and determined the micelle axial ratios, J, in such

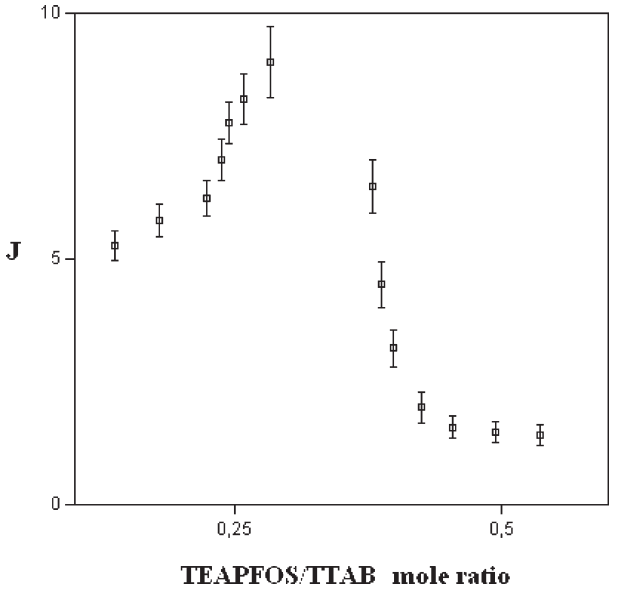

Figure 7. Dependence of axial ratios, *J*, calculated by eq 4, for 10.0 mmol *TTAB*/TEAPFOS mixtures in 25.0 mmol kg^{-1} TEABr vs the TEAPFOS/*TTAB* mole ratio. Low and stable *J* values on the right refer to vesicles.

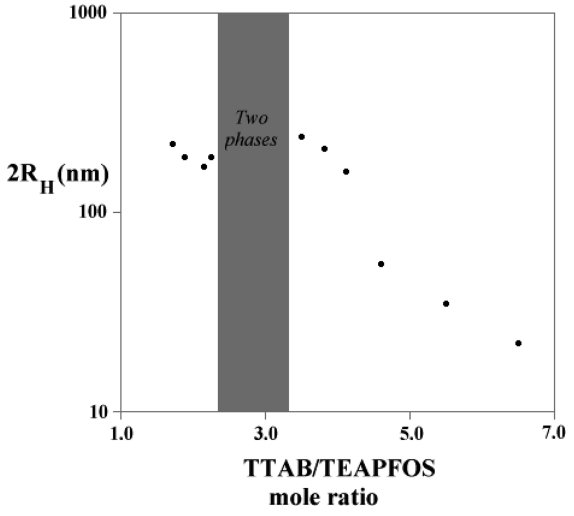

Figure 8. Average hydrodynamic diameters, $2R_H$, in nm, vs the TTAB/*TEAPFOS* mole ratio, at 25.0 °C. The overall surfactant content is 10.0 mmol and the amount of added TEABr 25.0 mmol kg^{-1}. DLS indicate the onset of large, spherical, aggregates below the 4.0/1.0 mol ratio threshold. Above it, anisometric entities occur. The two-phase area, in gray, was not investigated.

mixtures. The concentration dependence of axial ratios is reported in Figure 7. *J* was defined as[47]

$$\left(\frac{K_\eta - 2.5}{0.407}\right) = (J-1)^{1.509} \quad (4)$$

where K_η is a phenomenological shape factor, obtained by linearizing relative viscosity data. Equation 4 is useful when micelles are undefined in size and shape. In such case, the viscosity is expressed in terms of empirical relations based on either volume fraction or ellipticity.

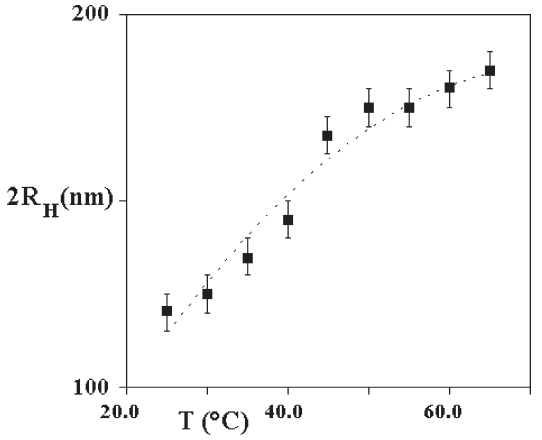

Figure 9. Plot of vesicle size, $2R_H$, in nm, as a function of *T*, in °C, for a 10.0 mmol kg^{-1} TTAB/TEAPFOS mixture, of mole ratio 1.5/1.0, in 25.0 mmol kg^{-1} TEABr. The dotted line is an eye-guide.

Nagarajan and Hammond[47] stated that, in low-concentration regimes and if intermicellar interactions are negligible, K_η is directly related to micellar shape. At quite high volume fractions, the relationship between K_η and micellar shape may be influenced by higher terms, due to the interactions between aggregates. At present, we do not know as to whether micelle shape is due to higher terms or anisotropy. Perhaps, the systems are diluted and we assume that any eventual effect is related to the anisotropy of such aggregates.

K_η experimental data were compared with those pertinent to spherical particles (2.5), and the excess value was assumed to be proportional to *J*. Data indicate that transitions to an-isometric entities occur above a given TEAPFOS/TTAB mole ratio (about 0.25). They also indicate the onset of a plateau, above the two-phase threshold of the dispersions, Figure 8, where angularly resolved *DLS* indicate the onset of spherical vesicles.

Hydrocarbon/fluorocarbon vesicles were formerly observed in mixtures of CTAB and sodium perfluorooctanoate (with 16 and 7 carbon atoms in the two chains, respectively), or CTAB and sodium perfluorohexanoate (with 5 CF_2 units).[48] Very presumably the length of poly methylene and polyfluoromethylene chains controls vesicle formation and stability. When the length ratio is higher than 1/2 (as in the present case), non ideality effects are more significant and vesicles are hardly formed.

Vesicle sizes are lower compared to the SDS/CTAB system (120 compared to 250), and the dispersions are turbid. This is a preliminary evidence on the occurrence of multilamellar entities, if we compare the present system with the SDS/CTAB one. SAXS data, not reported here, support the above hypothesis.[49] Thermal transitions occur in this system too, but the effect is much less significant than in the SDS/CTAB one. Vesicles sizes remain nearly constant up to 65.0 °C, and slightly increase above that limit, Figure 9. In that system, no multi- to unilamellar transitions are observed by raising *T*.

4. DISCUSSION

The two systems are different each from the other. The SDS/CTAB one forms multi and unilamellar vesicles, depending on thermal treatment. We noticed that the size of such vesicles is sensitive to added electrolytes. It is conceivable, thus, to suppose

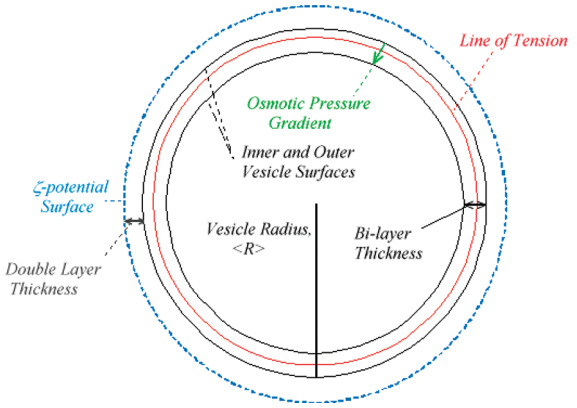

Figure 10. Model indicating the forces active on bilayer vesicles, in equilibrium conditions. The inner and outer vesicle surfaces are in black, the double-layer thickness in gray, the osmotic pressure gradient in green, the line of tension in red. The surface on which ζ-potential is measured is in blue.

that the osmotic pressure across the vesicle bilayers and their state of charge are influenced by addition of salt. In addition, vesicles are elastic. TTAB/TEAPFOS vesicles are always multilamellar in character and will not be considered in the following. The multilamellar state of TTAB/TEAPFOS vesicles, in fact, does not allow to determine the balance of forces in such systems.

4.1. Description of the Model. Equilibrium single unilamellar vesicles occurring in the SDS/CTAB system are the result of a complex balance between electrostatic, surface, elastic and osmotic terms. At equilibrium, the size of unilamellar vesicles is controlled by the combination of osmotic, $(\Delta\Pi/\nu\Delta c)$, electrostatic, $(-q\Psi^\circ)$, elastic, $(Kl^2/2$, where l is the maximum vesicle circumference), and surface work, (γA), contributions. A scheme of the model we have used is reported in Figure 10. The balance of energy contributions is discussed below.

In particular, $\Delta\Pi$, ν and Δc refer to the osmotic pressure gradient, concentration and number of ions acting normal to the bilayers. $\Delta\Pi$ gradient operates between $(\langle R_H\rangle - \delta)$ and $(\langle R_H\rangle + \delta)$, where δ is half the bilayer thickness (~2 nm) and $\langle R_H\rangle$ the average vesicle radius. The osmotic pressure gradient across vesicles is significant and concurs to reduce $2R_H$ values. This statement finds support from previously reported DLS and ζ-potential findings.

The bending elasticity term operates on a line of tension equivalent to the vesicle circumference. It is effective in three directions and is counted as $(3Kl^2/2)$, because the deformation of vesicles operates in three directions. l is the line of tension. In the surface energy term it should be counted as $2\gamma l^2$. The electrostatic term is active on the outer vesicle surface (l^2 is the area on which it operates). A visual picture of the model we have used is drawn in Figure 10.

Considering all the above contributions and dividing all terms by l makes possible to relate vesicle elasticity to all other terms, according to

$$\left(\frac{\Delta\Pi}{\nu\Delta\Gamma_i}\right) + 2\gamma l - \left(\frac{ql}{A}\right)\bar{\Psi}^\circ = \left(\frac{\Delta\Pi}{\nu\Delta\Gamma_i}\right) + 2\gamma l - \sigma\tau\bar{\Psi}^\circ = -\left(\frac{3Kl}{2}\right) \quad (5)$$

where $\Delta\Gamma_i$ is the excess of the ith species in the outer vesicle surface, and γl a surface force. $\Delta\Gamma_i$ in eq 5 refers to the anionic surfactant in excess, SDS. The $\sigma\tau$ term in eq 5 is an electric moment per unit area, times the electrostatic potential sensed by the vesicles, $\bar{\Psi}^\circ$. The double layer thickness, τ, depends on the medium ionic strength, and was formerly inferred from dielectric relaxation studies.[30,34] In the present experimental conditions, it ranges between 5 and 10 nm. We assume that cat/anionic vesicles conform to Smoluchowskj's approximation,[33] since τ is ≪ than the vesicle radius.

The surface charge density of vesicles can be calculated by the relation

$$\left(\frac{\sigma_s}{\sigma^\circ - \sigma_s}\right) = N_{\text{ion, exc}}\ \exp^{(ze\bar{\Psi}^\circ + \phi/k_B T)} \quad (6)$$

where $N_{\text{ion,exc}}$ is the concentration in excess of SDS with respect to CTAB, and ϕ is a non electric term. The term $(\sigma_s/\sigma^\circ - \sigma_s)$ in eq 6 is a surface charge density (it is the ratio of occupied to non occupied sites) and refers to SDS in excess. The free energy of the diffuse double layer around vesicles can be evaluated in terms of a reversible transformation from a charged state, in presence of double layer ions, to an uncharged surface plus normal ions in solution. It is evaluated by integrating the electrostatic surface work term, according to

$$G^S_{\text{elec}} = -\int_0^{\bar{\Psi}^\circ} \sigma d\bar{\Psi}^\circ \quad (7)$$

where σ can be expressed as

$$\sigma = \left(\frac{2N^\circ_{\text{ion, exc}}\varepsilon k_B T}{\pi}\right)^{1/2} \sinh\left(\frac{ze\bar{\Psi}^\circ}{2k_B T}\right) \quad (7')$$

Equation 7′ formally accounts for surface charge density terms.

4.2. Validation of the Model. To check the consistency of results calculated by eqs 6, 7, and 7′, experimental support is needed. In the following surface charge density terms, $\sigma\tau$ (inferred by ζ-potential), osmotic pressure contributions (calculated by the medium ionic strength), γ (inferred by surface tension), and elastic terms (taken from ref 48.) were considered. In particular, $\sigma\tau$ was determined by combining ζ-potentials and dielectric relaxation experiments.[30,34] We observed that σ values calculated from eqs 7 and 7′ are ~5% higher than those inferred from experiments. Thus, the agreement between experiments and theory for this contribution is fairly good.

When equilibrium between the above different forces takes place, and vesicle size are constant, the average vesicle radius, $\langle R\rangle$, can be quantified by the relation

$$l = 2\pi\langle R_H\rangle = \left[\frac{\sigma\tau\bar{\Psi}^\circ - \left(\frac{\Delta\Pi}{\nu\Delta\Gamma_i}\right)}{2\gamma + \left(\frac{3K}{2}\right)}\right] \quad (8)$$

which is obtained by arrangement of eq 5. Equation 8 accounts for all forces acting onto bilayers, and indicates that $\langle R\rangle$ depends on their balance.

Estimates on the validity of eq 8 were made by comparing experimental R_H values with computed ones. The former were measured in SDS/CTAB mixtures having 1.70/1.0 and 2.50/1.0 mol ratios, in presence of 50.0 mmol NaBr, or without it. The experimental size of thermally conditioned vesicles is close to 160−180 nm with 50.0 mmol NaBr and 200−250 nm without it.

To make possible a comparison between theory and experiments, we assumed that K in eq 8 is the same as in CTAB/SOS vesicles ($\sim 0.7 \pm 0.2\ k_BT$ units[48]). Presumably, its exact value is different from the one we have used. All other quantities in eq 8 were inferred from experiments, as indicated above. The computed results indicate that vesicle sizes in absence of added electrolyte span between 250 and 300 nm and 180−220 with 50.0 mmol added NaBr. The agreement between experiments and predicted values, thus, is good. eqs 5 and 8 make it possible to relate vesicle curvature to the forces acting on it and to get relevant results. To our knowledge, this is the first effort to relate bending elasticity to other terms. Not all contributions in eqs 5 and 8 are relevant, and the above relation can be simplified. This is true for osmotic pressure terms, when no added electrolyte is present.

It is interesting to compare the result by eq 8 with those predicted by Kaler for similar systems. He expressed the links between vesicle size and elasticity in terms of a curvature energy per unit area, f_c.[11,46,48] The approach he used is similar to that by Helfrich,[50] and others.[51,52] Accordingly, the spontaneous vesicles curvature, $\langle R \rangle$, came out from a proper relation between curvature modulus and saddle-splay one.[48] In Kaler's approach vesicle size is controlled by elastic terms only: in the present one, conversely, $\langle R \rangle$ is due to the balance of different forces and comparison is cumbersome.

5. CONCLUSIONS

In this contribution, we showed that vesicle sizes at equilibrium are centered around a certain value, which depends on temperature, surfactant content, and ionic strength.[53−55] Similar effects were also observed in lipid mixtures.[56] From a physicochemical viewpoint, there is no significant difference in vesicle formation when surfactants or lipids are mixed together. In fact, mixing in the bilayer occurs between two, three or four alkyl chains in fluid state. The only difference between lipid-based and surfactant-based vesicles is the respective solubility in molecular form and the differential entropy of transfer of the components.[57,58] In the present system, a high solubility of the surfactants gives rise to significant matter exchange and favors, in proper conditions, the onset of an equilibrium state.

Vesicle sizes in cat/anionic systems can be tuned if contributions due to elasticity, surface tension, osmotic pressure and electrostatic terms are properly balanced. To the best of our knowledge, this is the first effort along this line. It may help describing the resulting effects on sound physical grounds. The observed effects are related to composition, that is, to the chemical potentials of the species and can be tuned by increasing the relative amounts of each species, the medium ionic strength or raising the temperature to get unilamellar vesicles. The present results are in line with previous hypotheses on the spontaneous vesicle curvature.[57,58]

Practical applications of the above approach are of substantial interest in studies dealing with vesicles as carriers, in the encapsulation of drugs,[59] in the adsorption and release of *DNA* or other biopolymers, in transfection technologies.[60] The balance of forces active on unilamellar vesicles may be properly tuned to get carriers for in vitro and in vivo applications. Further investigation on the above items is of fundamental relevance, given the moderate cyto-toxicity of the above formulations.[61]

As to the performances that cat/anionic surfactant mixtures show, the present results indicate that fluorocarbon/hydrocarbon mixtures are less effective compared to hydrocarbon-based ones. The reasons for that behavior arise from a poor chemical compatibility (and poor ideality of mixing) and from the rigidity of fluorinated chains. Alternatives rely on using fluorocarbons with shorter chain lengths. Perhaps, the elastic bending constant of fluorocarbon/hydrocarbon mixtures is significantly high compared to the SDS/CTAB one.[48] Vesicles containing rigid molecules, thus, have different elastic performances compared to the SDS/CTAB system. Molecules with a high rotational freedom degree ensure a higher vesicles flexibility compared to those containing fluorocarbons, cholesterol, or rigid molecules. This implication needs further experimental evidence to be clarified.

To get bilayers, at least one amphiphile must be appreciably water-soluble. This is why they are hardly formed in lipid mixtures. There, the partitioning between vesicles and the bulk is much less effective than cat/anionic vesicles made of single chain species. For instance, bilayers are not obtained in sodium dodecylsulfate/didodecyldimethylammonium bromide mixtures,[62] even after prolonged thermal cycling. It is conceivable that single chain surfactants partition between unilamellar vesicles and the bulk more easily than double chain ones, because of solubility reasons.

AUTHOR INFORMATION

Corresponding Author

*Address: Dept. of Chemistry, Cannizzaro Building, La Sapienza University, P.le A. Moro 5, I-00185 Rome, Italy. E-mail: camillo.lamesa@uniroma1.it.

Notes

||Permanent Address: I.R.C.C.S. Foundation, Istituto Neurologica Carlo Besta, IFOM-IEO- Campus, Milan, Italy.

ACKNOWLEDGMENT

Thanks are due to La Sapienza University for financing the present project through a Faculty project. The authors are strongly indebted to Prof. Gianfranco Risuleo (Dept. of Molecular Biology) and Professor Adalberto Bonincontro (Dept. of Physics), at La Sapienza University, for many fruitful and useful discussions during the preparation of this manuscript. We thank the reviewers for cogent and fruitful criticism on some aspects of the manuscript. Their anonymous work was greatly appreciated.

REFERENCES

(1) Tucker, I.; Penfold, J.; Thomas, R. K.; Grillo, I.; Barker, J. G.; Mildner, D. F. R. *Langmuir* **2008**, *24*, 7674–7687.

(2) Dong, S.; Xu, G.; Hoffmann, H. *J. Phys. Chem. B* **2008**, *112*, 9371–9378.

(3) Weiss, T. M.; Narayanan, T.; Gradzielski, M. *Langmuir* **2008**, *24*, 3759–3766.

(4) Blanco, E.; Messina, P.; Ruso, J. M.; Prieto, G; Sarmiento, F. *J. Phys. Chem. B* **2006**, *110*, 11369–11376.

(5) Kronberg, B. *Curr. Opin. Colloid Interface Sci.* **1997**, *2*, 456–463.

(6) Somasundaran, P.; Huang, L. *Adv. Colloid Interface Sci.* **2000**, *88*, 179–208.

(7) Sakai, K.; Matsuhashi, K.; Honya, A.; Oguchi, T.; Sakai, H.; Abe, M. *Langmuir* **2010**, *26*, 17119–17125.

(8) Hill, R. M. *Mixed Surfactant Systems*, Surfactant Science Series 46; M. Dekker: New York, 1992; pp 317−339.

(9) Scamehorn, J. F.; Harwell, J. H. *Mixed Surfactant Systems*, Surfactant Science Series 46; M. Dekker: New York, 1992; pp 283−315.

(10) Ninham, B. W.; Evans, D. F. *Faraday Discuss. Chem. Soc.* **1986**, *81*, 1–17.
(11) Anraku, Y.; Kishimura, A.; Oba, M.; Yamasaki, Y.; Kataoka, K. *J. Am. Chem. Soc.* **2010**, *132*, 1631–1636.
(12) Kaler, E. W.; Herrington, K. L.; Zasadzinski, J. A. N. *Mater. Res. Soc. Symp. Proc.* **1992**, *248*, 3–10.
(13) Nilsson, U.; Joensson, B.; Wennerstroem, H. *J. Phys. Chem.* **1993**, *97*, 5654–5660.
(14) Shen, Y.; Hao, J.; Hoffmann, H.; Wu, Z. *Soft Matter* **2008**, *4*, 805–810.
(15) Marques, E. F.; Regev, O.; Khan, A.; Lindman, B. *Adv. Colloid Interface Sci.* **2003**, *100−102*, 83–104.
(16) Zhang, J.; Song, A.; Li, Z.; Xu, G.; Hao, J. *J. Phys. Chem. B* **2010**, *114*, 13128–13135.
(17) Walker, S. A.; Zasadzinski, J. A. *Langmuir* **1997**, *13*, 5076–5081.
(18) Marques, E. F. *Langmuir* **2000**, *16*, 4798–4807.
(19) Engberts, J. B.; Kevelam, J. *Curr. Opin. Colloid Interface Sci.* **1996**, *1*, 779–789.
(20) Tondre, C.; Caillet, C. *Adv. Colloid Interface Sci.* **2001**, *93*, 115–134.
(21) Bonincontro, A.; Spigone, E.; Ruiz Pena, M.; Letizia, C.; La Mesa, C. *J. Colloid Interface Sci.* **2006**, *304*, 342–347.
(22) Gente, G.; La Mesa, C.; Muzzalupo, R.; Ranieri, G. A. *Langmuir* **2000**, *16*, 7914–7919.
(23) Andreozzi, P.; Funari, S. S.; La Mesa, C.; Mariani, P.; Ortore, M. G.; Sinibaldi, R.; Spinozzi, F. *J. Phys. Chem. B* **2010**, *114*, 8056–8060.
(24) Mel'nikov, S. M.; Dias, R.; Mel'nikova, Y. S.; Marques, E. F.; Miguel, M. G.; Lindman, B. *FEBS Lett.* **1999**, *453*, 113–118.
(25) Fischer, A.; Hebrant, M.; Tondre, C. *J. Colloid Interface Sci.* **2002**, *248*, 163–168.
(26) Lohse, B.; Bolinger, P.-Y.; Stamou, D. *J. Am. Chem. Soc.* **2008**, *130*, 14372–14373.
(27) Rico, A.; Lattes, I. *J. Phys. Chem.* **1986**, *90*, 5870–5874.
(28) La Mesa, C.; Coppola, L. *Colloids Surf.* **1989**, *35*, 325–328.
(29) Vautrin, C.; Zemb, T.; Schneider, M.; Tanaka, M. *J. Phys. Chem. B* **2004**, *108*, 7986–7991.
(30) Andreozzi, P.; Bonincontro, A.; La Mesa, C. *J. Phys. Chem. B* **2008**, *112*, 3339–3345.
(31) Koppel, D. E. *J. Chem. Phys.* **1972**, *57*, 4814–4820.
(32) Provencher, S. W. *Comput. Phys. Commun.* **1982**, *27*, 213–218.
(33) Adamson, A. W. *Physical Chemistry of Surfaces*, 5th ed.; Wiley & Sons: New York, 1990; Chapter V, p 203.
(34) Letizia, C.; Andreozzi, P.; Scipioni, A.; La Mesa, C.; Bonincontro, A.; Spigone, E. *J. Phys. Chem. B* **2007**, *111*, 898–908.
(35) *Handbook of Chemistry and Physics*, 61th ed.; CRC Press: Boca Raton, FL, 1980; Table F45.
(36) Almgren, M.; Wang, K.; Asakawa, T. *Langmuir* **1997**, *13*, 4535–4344.
(37) Alam, T. M.; McIntyre, S. K. *Langmuir* **2008**, *24*, 13890–15896.
(38) Mukerjee, P.; Handa, T. *J. Phys. Chem.* **1981**, *85*, 2298–2303.
(39) Mukerjee, P.; Korematsu, K.; Okawauchi, M.; Sugihara, G. *J. Phys. Chem.* **1985**, *89*, 5308–5312.
(40) Mysels, K. J. *J. Colloid Interface Sci.* **1978**, *66*, 331–334.
(41) Penfold, J.; Staples, E.; Thompson, L.; Tucker, I.; Thomas, R. K.; Lu, J. R. *Ber. Bunsen-Gesell. Phys. Chem.* **1996**, *100*, 218–223.
(42) Shinoda, K.; Nomura, T. *J. Phys. Chem.* **1980**, *84*, 365–369.
(43) Mukerjee, P.; Yang, A. Y. S. *J. Phys. Chem.* **1976**, *80*, 1388–1390.
(44) Ciurleo, A.; Cinelli, S.; Guidi, M.; Bonincontro, A.; Onori, G.; La Mesa, C. *Biomacromolecules* **2007**, *8*, 399–405.
(45) Vand, V. *J. Phys. Chem. Colloid* **1948**, *52*, 277–299.
(46) Fontell, K. *Koll. Z. Z. Polym.* **1971**, *246*, 614–625.
(47) Nagarajan, R.; Hammond, S. *Colloids Surf.* **1982**, *1*, 162–181.
(48) Jung, H. T.; Coldren, B.; Zasadzinski, J. A.; Iampietro, D. J.; Kaler, E. W. *Proc. Nat. Acad. Sci. U.S.A.* **2001**, *98*, 1353–1357.
(49) Ortore, M. G. Private communication.
(50) Helfrich, W. *Zh. Naturforsh. A* **1978**, *33*, 305–315.
(51) Bergstrom, L. M. *J. Colloid Interface Sci.* **2006**, *293*, 181–183.
(52) Bergstrom, M. *Langmuir* **2001**, *17*, 7675–7686.
(53) Hentze, H.-P.; Raghavan, S. R.; McKelvey, C. A.; Kaler, E. W. *Langmuir* **2003**, *19*, 1069–1074.
(54) Silva, B. F. B.; Marques, E. F.; Olsson, U. *Langmuir* **2008**, *24*, 10746–10754.
(55) Marques, E. F.; Brito, R. O.; Silva, S. G.; Rodriguez-Borges, J. E.; do Vale, M. L.; Gomes, P.; Araujo, M. J.; Soderman, O. *Langmuir* **2008**, *24*, 11009–11017.
(56) Lozano, N.; Pinazo, A.; La Mesa, C.; Perez, L.; Andreozzi, P.; Pons, R. *J. Phys. Chem. B* **2009**, *113*, 6321–6327.
(57) Safran, S. A.; Pincus, P. A.; Andelman, D.; MacKintosh, F. C. *Phys. Rev. A* **1991**, *43*, 1071–1078.
(58) MacKintosh, F. C.; Safran, S. A. *Phys. Rev. E* **1993**, *47*, 1180–1185.
(59) Dey, S.; Mandal, U.; Sen Mojumdar, S.; Mandal, A. K.; Bhattacharyya, K. *J. Phys. Chem. B* **2010**, *114*, 15506–15511.
(60) Bonincontro, A.; La Mesa, C.; Proietti, C.; Risuleo, G. *Biomacromolecules* **2007**, *8*, 1824–1829.
(61) Aiello, C.; Andreozzi, P.; La Mesa, C.; Risuleo, G. *Colloids Surf. B: Biointerfaces* **2010**, *78*, 149–154.
(62) Pucci, C., Thesis, 2010.